DFT investigation of toluene adsorption on silicon carbide nanosheet doping with transition metal for storage and sensor application

Pasakorn Sangnikul[1*], Chanukorn Tabtimsai[1,], Wandee Rakrai[1], Banchob Wanno[2]**

[1] Computational Chemistry Center for Nanotechnology and Department of Chemistry, Faculty of Science and Technology, Rajabhat Maha Sarakham University, Maha Sarakham 44000, Thailand

[2] Center of Excellence for Innovation in Chemistry and Supramolecular Chemistry Research Unit, Department of Chemistry, Faculty of Science, Mahasarakham University, Maha Sarakham 44150, Thailand

Corresponding author e-mail: *champ9yod@gmail.com,tabtimsai.c@gmail.com**

Abstract

Nowadays, the emission of volatile organic compounds (VOC) is giving rise to several health hazards and damage to the environment. Consequently, the nanomaterial development is considerably important for VOC adsorption and sensing. In this work, the adsorptions of toluene on silicon carbide nanosheets doping with transition metal atoms (TM-doped SiCNS) were investigated using the density functional theory method (DFT). The B3LYP/LanL2DZ was employed in all calculations for the geometric, energetic, and electronic properties. In addition, the doping of TM atom at different sites will have different effects on the adsorption behavior of the systems. Calculation results reveal that the adsorption distances and adsorption energies of TM doping on SiCNSs are suitable for toluene adsorption greater than pristine SiCNS. According to the changes of electronic properties of TM-doped SiCNS show highly sensitive to toluene molecule. The results indicate that the introducing of TM doping on SiCNS significantly improve the sensitivity toward toluene molecule. Therefore, the results of our work may be useful in developing and designing new types of storage and sensor materials.

Keywords: DFT, Silicon carbide nanosheet, Toluene, Transition metals, VOC

_____

1. Introduction

Volatile organic compounds (VOC) are common air pollutants emitted by the chemical industries such as production of adhesives, paints, printing materials, building materials, and chemicals for synthesis (Kim et al., 2019). For this reason, it is an important issue to develop sensors for detect and manage VOC. In the recent year, the experimental and theoretical studies about VOC adsorption on different nanostructures have been reported widely (Chiang et al., 2001; Su et al., 2018). Manaschai Kunaseth et al. have investigated the adsorption of VOC on transition metal deposited graphene which adsorption energy of benzene was -1.93 eV calculated by using Perdew-Wang functional (PW91) (Kunaseth et al., 2017). The para-nitrophenol molecule adsorption on vacancy and Pt-doped graphene sheets showed that the adsorption capacity of graphene can be significantly increased (Mandeep et al., 2018). Toluene is volatile organic compound that evaporate at room temperature. Toluene is harmful to human health, and may cause various diseases such as headache, nausea, coryza,

pharyngitis, emphysema, lung cancer, and even death (Yi et al., 2008). Also study of the adsorptions of VOCs on activated carbon/metal oxide composites have been performed by Ke Zhou et al, that calculation shows that the highest adsorption energy of toluene on activated carbon was -20.87 kJ/mol calculated by using JW-BK132Z functional (Zhou et al., 2019). Lian Yu et al. have reported the adsorption of VOC on reduced graphene oxide, and the results suggested that graphene oxide is excellent adsorption performance for toluene molecule (Yu et al., 2018). As previously mentioned, Experimental and theoretical studies on the adsorption of VOC are showed extremely interesting and it is necessary to understand more.

The silicon carbide nanosheet (SiCNS) has recently attracted considerable attention due to it has the notable properties such as thermal stability, chemical inertness, high thermal conductivity, and others (Delavari & Jafari., 2018; Ansari et al., 2013).
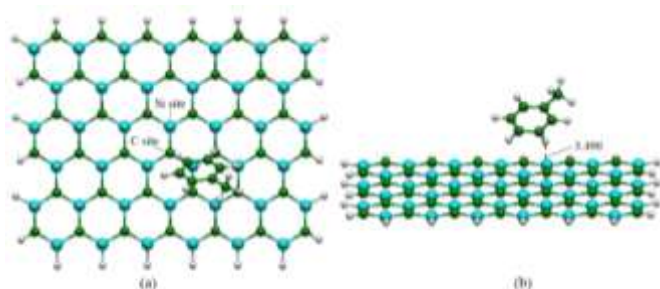
Figure 1. The B3LYP/LanL2DZ optimized structures of top views of (a) pristine SiCNS and (b) toluene adsorbed on pristine SiCNS

They also have wide range of applications in different fields such as energy conversion, enhance materials strength, gas storage and sensing applications (Chabi et al., 2016). However, pristine SiCNS has been explored as low efficient for adsorption or storage and low sensitive to small molecule (Wang et al., 2016). Therefore, many studies are devoted to improving the surface sensibility of silicon carbide nanostructures by introducing doping metal atoms. Doping of transition metal (TM=Fe, Co, Al, Cu, and Zn) atoms on SiCNS can improve the adsorption abilities of TM-doped SiCNS to small molecule and change electronic properties of TM-doped SiCNS (Sun et al., 2016). Ga- and B-doped SiCNSs show better capability of small molecule adsorption capability than undoped SiCNS (Tabtimsai et al., 2015). The silicon carbide nanotube (SiCNT) doping with group 8B transition metal are appropriate for hydrogen storage and show better hydrogen adsorption capability than undoped SiCNT (Tabtimsai et al., 2018).

To the best of our knowledge, there are no reports the adsorption abilities of toluene molecule on TM-doped SiCNS. Therefore, aim of this work, we investigate the geometric, energetic, and electronic properties of pristine and TM-doped SiCNSs by density functional theory (DFT) and subsequently we evaluate their ability in adsorption of toluene molecules.

2. Computational details

The structure optimization of SiCNS ($C_{39}Si_{39}H_{24}$) was modeled and used. The edges of the sheet were saturated by hydrogen atoms to avoid the boundary effects. The doping of TM atom on the center of SiCNS was modeled. The transition metal atoms, i.e., V, Nb, Ta, Cr, Mo, W, Mn, Tc, and Re were doping on carbon (TM_C) or silicon (TM_{Si}) atom at the center of SiCNS. Therefore, systems of TM-doped on SiCNS were considered the spin-polarized restricted and unrestricted optimizations. Geometrical optimizations of their systems were taken under the DFT calculation. The calculation was performed under hybrid density functional B3LYP, Becke's three parameter exchange functional with the Lee-Yang-Parr correlation functional (B3LYP) (Becke., 1988, 1993; Lee., 1988) and the Los Alamos LanL2DZ split-valence basis set (Hay & Wadt., 1985a, 1985b). All calculations were performed by using GAUSSIAN 09 program (Frisch et al., 2009). The geometrical parameters as equilibrium structural and natural bond orbitals (NBO) charges of studied compounds were specified at T= 0 K. The molecular graphics of all related species were generated with the MOLEKEL 4.3 program (Flükiger et al., 2000). The electronic density of states (DOSs) of all systems were plotted by the GaussSum 2.2 program (O'boyle et al., 2008). Adsorption energy (E_{ads}) of toluene
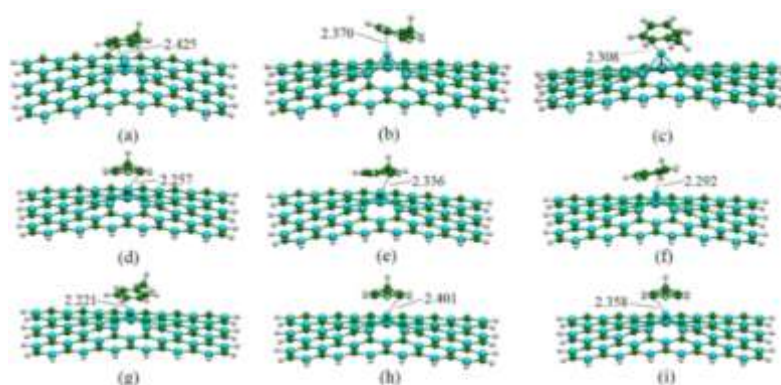

Figure 2. The B3LYP/LanL2DZ optimized structures of toluene adsorbed on TM_C-SiCNSs, (a) toluene/V_C-, (b) toluene/Nb_C-, (c) toluene/Ta_C-, (d) toluene/Cr_C-, (e) toluene/Mo_C-, (f) toluene/W_C-, (g) toluene/Mn_C-, (h) toluene/Tc_C-, and (i) toluene/Re_C-doped SiCNSs.
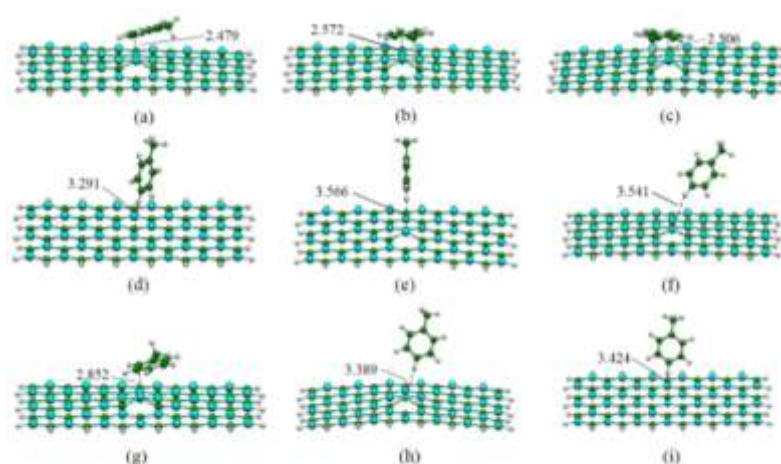
15

Figure 3. The B3LYP/LanL2DZ optimized structures of toluene adsorbed on TM_{Si}-SiCNSs (a) toluene/V_{Si}-,(b) toluene/Nb_{Si}-, (c) toluene/Ta_{Si}-, (d) toluene/Cr_{Si}- (e) toluene/Mo_{Si}- (f) toluene/W_{Si}- (g) toluene/Mn_{Si}- (h) toluene/Tc_{Si}-, and (i) toluene/Re_{Si}-doped SiCNSs.

molecule adsorbed on the pristine and TM-doped SiCNS were obtained from equations

$$E_{ads} = E_{toluene/SiCNS \text{ or } TM\text{-}SiCNS} - (E_{SiCNS \text{ or } TM\text{-}SiCNS} + E_{toluene}) \qquad (1)$$

, where $E_{toluene/SiCNS \text{ or } TM\text{-}SiCNS}$ are the total energy of the adsorption of toluene molecule on pristine or TM-doped SiCNS. The $E_{SiCNS \text{ or } TM\text{-}SiCNS}$ and $E_{toluene}$ are the total energies of pristine or TM-doped SiCNS and toluene molecule, respectively. Considering the electronic properties in term of the highest occupied molecular orbital energies (E_{HOMO}), the lowest unoccupied molecular orbital energies (E_{LUMO}), the energy gaps (E_{gap}) referred to the energy difference between HOMO and LUMO orbitals and changes of energy gaps (ΔE_{gap}) referred to the gap difference between before and after gas adsorption were investigated at the same theoretical level.

3. Results and discussion
3.1 Geometrical structures
The B3LYP/LanL2DZ-optimized structures of the pristine and their adsorption with toluene molecule are displayed in Fig. 1. In addition, the doping sites are showed in Fig.1a. The calculated average Si-C bond lengths and bond angles of pristine SiCNS are found to be 1.780 Å and 120.0º, respectively, which are in accordance with the previous reports (Delavari & Jafari., 2018). The bond lengths, bond angles, and adsorption distances of toluene adsorbed on pristine, V-, Nb-, Ta-, Cr-, Mo-, W-, Mn-, Tc-, and Re-doped SiCNSs are listed in Table 1. In comparison of pristine SiCNS with the toluene adsorbed on pristine SiCNS

(toluene/SiCNS), the bond lengths and bond angles of pristine SiCNS system are slightly changed. Therefore, toluene/SiCNS reflected that toluene molecule occur the weak interaction.

The toluene adsorptions on TM_C-SiCNS (toluene/TM_C-SiCNS) are showed in Fig 2., the Si-TM bond lengths are in the ranges of 2.294-2.563 Å, while the Si-TM-Si bond angles are in the ranges of 78.6-97.3º. Obviously, after toluene adsorption, the surface of TM_C-SiCNS still reveal the protruded geometrical structures which were similar trends can be found in other works (Farmanzadeh & Ardehjani., 2018). In another hand, the B3LYP/LanL2DZ-optimized structures of toluene/TM_{Si}-SiCNS are displayed in Fig 3. The C-TM bond lengths of toluene/TM_{Si}-SiCNS obtained in this study are in the ranges of 1.825 - 2.035 Å, which are significantly shorter than C-TM of TM_C-SiCNS, while the bond angles of C-TM-C at the doping site of toluene/$TM_{Si}SiCNS_{Si}$ are in the range of 107.5 - 121.0º, which were wider than that of the Si-TM-Si bond angles of toluene/TM_C-SiCNS.

The adsorption distances (AD) between toluene molecule and pristine SiCNS or TM-doped SiCNS are listed in Table 1. The AD between toluene molecule and the pristine SiCNS is calculated to be 3.490 Å. The AD between the toluene molecule and TM-SiCNSs are found in the range 2.234-2.476 and 2.479-3.566 Å for TM_C-SiCNS and TM_{Si}-SiCNS, respectively. This indicates that interactions between toluene molecule and TM_C-SiCNS are stronger than TM_{Si}-SiCNS.

Table 1. The selected geometrical parameters and adsorption distances (AD) of toluene molecule adsorbed on pristine and TM-doped SiCNS.

Species	Si1-TM or C1-TM (Å)	Si2-TM or C2-TM (Å)	Si3-TM or C3-TM (Å)	Si1-TM-Si2 or C1-TM-C2 (°)	Si1-TM-Si3 or C1-TM-C3 (°)	Si2-TM-Si3 or C2-TM-C3 (°)	AD (Å)
toluene/SiCNS	1.798 [a]	1.824 [a]	1.798 [a]	119.3 [a]	121.2 [a]	119.3 [a]	3.490
toluene/V$_C$-SiCNS	2.464	2.481	2.465	83.3	86.1	83.4	2.476
toluene/Nb$_C$-SiCNS	2.513	2.546	2.510	84.3	85.0	78.5	2.370
toluene/Ta$_C$-SiCNS	2.554	2.534	2.546	82.4	81.4	83.1	2.309
toluene/Cr$_C$-SiCNS	2.415	2.315	2.311	80.9	85.0	96.4	2.234
toluene/Mo$_C$-SiCNS	2.398	2.563	2.393	80.6	94.5	79.9	2.336
toluene/W$_C$-SiCNS	2.437	2.479	2.426	81.5	88.6	86.4	2.292
toluene/Mn$_C$-SiCNS	2.294	2.310	2.320	91.0	87.9	86.7	2.267
toluene/Tc$_C$-SiCNS	2.355	2.427	2.353	85.2	92.0	85.2	2.473
toluene/Re$_C$-SiCNS	2.368	2.427	2.368	85.5	91.4	85.5	2.358
toluene/V$_{Si}$-SiCNS	1.891	1.983	1.884	109.2	115.2	109.6	2.479
toluene/Nb$_{Si}$-SiCNS	1.986	2.035	1.982	107.6	108.3	107.5	2.572
toluene/Ta$_{Si}$-SiCNS	1.978	2.023	1.982	107.5	108.5	107.6	2.506
toluene/Cr$_{Si}$-SiCNS	1.825	1.883	1.825	119.4	121.0	119.4	3.291
toluene/Mo$_{Si}$-SiCNS	1.932	1.982	1.930	113.2	114.5	113.1	3.566
toluene/W$_{Si}$-SiCNS	1.933	1.964	1.933	116.9	116.9	116.9	3.541
toluene/Mn$_{Si}$-SiCNS	1.938	1.972	1.938	109.2	112.5	109.4	2.852
toluene/Tc$_{Si}$-SiCNS	1.938	1.972	1.938	110.2	111.2	110.3	3.389
toluene/Re$_{Si}$-SiCNS	1.880	1.914	1.880	120.3	119.3	120.3	3.424

[a] Bond lengths and bond angles of toluene adsorbed on pristine SiCNS

3.2 Adsorption abilities of pristine and TM-doped SiCNSs onto toluene adsorbed

The adsorption energies (E_{ads}) of toluene adsorbed on the pristine, V-, Nb-, Ta-, Cr-, Mo-, W-, Mn-, Tc-, and Re-doped SiCNSs are listed in Table 2. The adsorption energy of toluene adsorbed on pristine SiCNS is -0.416 kcal/mol. This confirms that pristine SiCNS is slightly sensitive to toluene molecule. The adsorption energies of toluene adsorbed on TM$_C$-doped SiCNS are in a range of -51.604 and -30.922 kcal/mol. Their E_{ads} are in the following order: toluene/W$_C$-SiCNS (-51.604 kcal/mol) > toluene/Cr$_C$-SiCNS (-46.172 kcal/mol) > toluene/Mo$_C$-SiCNS (-41.204 kcal/mol) > toluene/Ta$_C$-SiCNS (-40.483 kcal/mol) > toluene/Mn$_C$-SiCNS (-38.511 kcal/mol) > toluene/Re$_C$-SiCNS (-35.833 kcal/mol) ≈ toluene/V$_C$-SiCNS (-35.583 kcal/mol) ≈ toluene/Nb$_C$-SiCNS (-35.469 kcal/mol) > toluene/Tc$_C$-SiCNS (-30.922 kcal/mol). The parameters of adsorption energies indicate that the TM$_C$-SiCNS are exothermic reactions. Surprisingly, the TM doping on C site significantly improved adsorption ability of SiCNS. The large adsorption energies and short AD reflected that toluene

molecule underwent the strong interaction with TM$_C$-doped SiCNS. These adsorption energies were in according to concordance with the previous studies (Su et al., 2018).

The adsorption energies of toluene adsorbed on TM$_{Si}$-doped SiCNS are also exothermic reactions which are in the range of -34.004 to -0.027 kcal/mol. Their E_{ads} order is found as follow: toluene/Mn$_{Si}$-SiCNS (-34.004 kcal/mol) > toluene/Ta$_{Si}$-SiCNS (-14.721 kcal/mol) ≈ toluene/Nb$_{Si}$-SiCNS (-13.747 kcal/mol) > toluene/V$_{Si}$-SiCNS (-5.815 kcal/mol) > toluene/Re$_{Si}$-SiCNS (-1.060 kcal/mol) ≈ toluene/Cr$_{Si}$-SiCNS (-1.021 kcal/mol) ≈ toluene/W$_{Si}$-SiCNS (-0.997 kcal/mol) > toluene/Mo$_{Si}$-SiCNS (-0.027 kcal/mol). The TM doping on Si site also improved adsorption ability of SiCNS. Therefore, the Mn$_{Si}$-SiCNS, Ta$_{Si}$-SiCNS, Nb$_{Si}$-SiCNS and V$_{Si}$-SiCNS are suitable adsorption energies and short AD that toluene molecule underwent the strong interaction with TM$_{Si}$-doped SiCNS. Except for the Re$_{Si}$-SiCNS, Cr$_{Si}$-SiCNS, W$_{Si}$-SiCNS, Mo$_{Si}$-SiCNS, and Tc$_{Si}$-SiCNS display the small adsorption energies, and large AD reflected that toluene molecule underwent the weak

Table 2. Adsorption energies (E_{ads}), E_{HOMO}, E_{LUMO}, E_{gap}, ΔE_{gap}, and partial charge transfers (PCT) of toluene molecule adsorbed on pristine and TM-doped SiCNSs, computed at the B3LYP/LanL2DZ level of theory.

Species	E_{ads} (kcal/mol)	E_{HOMO} (eV)	E_{LUMO} (eV)	E_{gap} (eV)	ΔE_{gap} (eV)	PCT (e)
toluene/SiCNS	-0.416	-3.919	-3.728	0.190	0.027	0.007
toluene/V_C-SiCNS	-35.583	-4.027	-3.293	0.735	-0.408	0.341
toluene/Nb_C-SiCNS	-35.469	-3.973	-3.728	0.245	0.218	0.162
toluene/Ta_C-SiCNS	-40.483	-4.055	-3.565	0.490	-0.245	0.052
toluene/Cr_C-SiCNS	-46.172	-3.837	-3.646	0.190	0.000	0.448
toluene/Mo_C-SiCNS	-41.204	-3.837	-3.619	0.218	-0.082	0.437
toluene/W_C-SiCNS	-51.604	-3.864	-3.646	0.218	0.109	0.303
toluene/Mn_C-SiCNS	-38.511	-4.082	-3.265	0.816	-0.082	0.414
toluene/Tc_C-SiCNS	-30.922	-4.055	-3.456	0.599	-0.109	0.283
toluene/Re_C-SiCNS	-35.833	-3.837	-3.646	0.190	0.000	0.204
toluene/V_{Si}-SiCNS	-5.815	-4.055	-3.374	0.680	0.163	0.204
toluene/Nb_{Si}-SiCNS	-13.747	-3.782	-3.402	0.381	0.463	0.212
toluene/Ta_{Si}-SiCNS	-14.721	-3.755	-3.402	0.354	0.490	0.236
toluene/Cr_{Si}-SiCNS	-1.021	-3.973	-3.755	0.218	0.000	-0.092
toluene/Mo_{Si}-SiCNS	-0.708	-3.973	-3.755	0.218	-0.027	-0.002
toluene/W_{Si}-SiCNS	-0.997	-3.973	-3.755	0.218	0.000	-0.002
toluene/Mn_{Si}-SiCNS	-34.004	-4.163	-3.347	0.816	-0.027	0.155
toluene/Tc_{Si}-SiCNS	7.531	-4.163	-3.402	0.762	0.163	0.003
toluene/Re_{Si}-SiCNS	-1.060	-3.919	-3.538	0.381	0.136	0.001

interaction. Whereas, the toluene adsorbed on Tc_{Si}-SiCNS (7.531 kcal/mol) is the endothermic reaction. Apparently, the adsorption ability of SiCNS onto toluene molecule is improved by TM doping which is similar with that of adsorption of volatile organic compounds onto Al-doped C_2N monolayer (19), and volatile organic compounds adsorption on transition metal deposited graphene (Chiang et al., 2001).

3.3 Electronic properties for the systems

To further investigate the adsorption phenomenon of the toluene molecule on the pristine and TM-doped SiCNSs is investigated, then we consider the E_{HOMO}, E_{LUMO}, E_{gap}, and ΔE_{gap} of the stable configuration of toluene molecule absorbed on pristine and TM-doped SiCNSs. In Table 2, theoretical calculation reveals that the E_{gap} of toluene/SiCNS is 0.190 eV. The E_{gap} of toluene/TM_C- and TM_{Si}-SiCNSs are in the range of 0.816 to 0.190 and 0.762 to 0.218 eV, respectively, which are smaller than the E_{gap} of pristine SiCNS (E_{gap} = 2.49 eV). For the pristine SiCNS, V_C-SiCNS, Nb_C-SiCNS, Ta_C-SiCNS, Mo_C-SiCNS, W_C-SiCNS, Mn_C-SiCNS, Tc_C-SiCNS, V_{Si}-SiCNS, Nb_{Si}-SiCNS, Ta_{Si}-SiCNS, Mo_{Si}-SiCNS, Mn_{Si}-SiCNS, Tc_{Si}-SiCNS, and Re_{Si}-SiCNS systems, the E_{gap} are changed by toluene adsorption, meaning the electronic properties of the systems are also

exponentially changed. The reducing of E_{gap} of TM-doped SiCNS due to toluene adsorption is in excellent agreement with the previous calculated results of TM-doped SiCNS (Farmanzadeh & Ardehjani., 2018). Except for toluene adsorption on Cr_C-SiCNS, Re_C-SiCNS, Cr_{Si}-SiCNS, and W_{Si}-SiCNS, the E_{gap} are not change.

The partial charge transfers (PCT) between toluene molecule and SiCNS were calculated. The loss and gain of electrons could also be determine
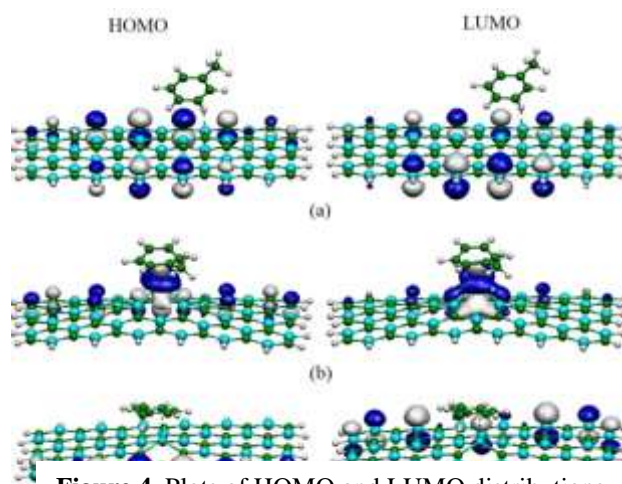
Figure 4. Plots of HOMO and LUMO distributions of (a) toluene/SiCNS, (b) toluene/Ta_C-SiCNS, and (c) toluene/Ta_{Si}-SiCNS.
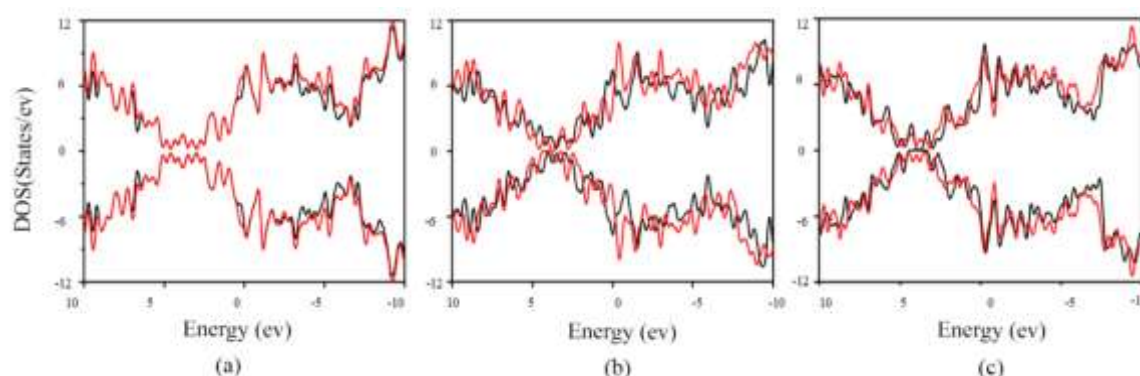
Figure 5. DOSs of (a) pristine SiCNS and toluene/SiCNS, (b) Ta_C-SiCNS and toluene/Ta_C-SiCNS, and (c) Ta_{Si}-SiCNS and toluene/Ta_{Si}-SiCNS. Before and after toluene adsorption are black and red lines, respectively.

by natural bond orbital (NBO) charge calculations before and after toluene adsorptions (Table 3). The PCT was defined as $Q_{toluene/SiCNS}$ - $Q_{toluene}$, where $Q_{touene/SiCNS}$ is the total charge of toluene adsorbed on pristine and TM-doped SiCNS, and $Q_{toluene}$ is the charge of toluene in free case. We found that the PCTs between toluene molecule and pristine SiCNS is about -0.007 e. The PCTs between toluene molecule and TM_C-SiCNS are in the ranges of 0.052 - 0.448 e. While the PCTs between toluene molecule and Mn_{Si}-SiCNS, Ta_{Si}-SiCNS, Nb_{Si}-SiCNS and V_{Si}-SiCNS are in the ranges of 0.236 - 0.155 e corresponding with strong adsorption abilities. The PCTs indicate that the large charge transfers between toluene molecule and TM_C-SiCNS and Mn_{Si}-SiCNS, Ta_{Si}-SiCNS, Nb_{Si}-SiCNS and V_{Si}-SiCNS are strongly bond due to covalent interaction. The covalent interaction between toluene molecule and TM-doped SiCNS is strong hybridization between the C's *p* orbital or H's *s* orbital of toluene and TM *d* orbital of TM-doped SiCNS. For the PCTs of toluene/TM_{Si}-SiCNS system, the PCTs between toluene molecule and Re_{Si}-SiCNS, Cr_{Si}-SiCNS, W_{Si}-SiCNS, Mo_{Si}-SiCNS, and Tc_{Si}-SiCNS are in the ranges of 0.001 to -0.092 e corresponding with weak adsorption abilities. Therefore, computations demonstrate that weak adsorption abilities of pristine SiCNS, Re_{Si}-SiCNS, Cr_{Si}-SiCNS, W_{Si}-SiCNS, Mo_{Si}-SiCNS, and Tc_{Si}-SiCNS slightly sensitive to toluene molecule.

Moreover, the HOMO and LUMO orbital distributions of the toluene adsorptions on pristine and TM-doped SiCNSs are also reported. The results show that, for toluene/SiCNS and toluene/TM_{Si}-SiCNS systems, the HOMO and LUMO orbitals are localized around the sheet (Figs. 4a and 4c.). Whereas, the HOMO and LUMO orbitals of TM_C-SiCNS are localized on the adsorption sites. The localization of the HOMO and LUMO orbitals of the toluene/Ta_C-SiCNS is clearly clustered (Fig. 4b.).

These results indicating the electron conduction through these systems.

The density of states were (DOSs) also calculated and plotted. The DOSs of pristine and TM-doped SiCNSs before and after toluene adsorption are displayed in Fig. 5. The DOSs of pristine SiCNS are slightly changed by toluene adsorption. This confirms that toluene molecule has slightly sensible effect on the electronic properties of the pristine SiCNS (Fig. 5a.). However, the DOSs of TM-doped SiCNS such as Ta_C-and Ta_{Si}-doped SiCNSs are significantly changed by toluene adsorption. These results are similar with Fe-doped SiCNS, reported by D. Farmanzadeh & Ardehjani (Farmanzadeh & Ardehjani., 2018). The changes of the DOSs are expected to bring about obvious changes in the corresponding electronic properties.

In summary, the adsorptions abilities of TM-doped SiCNS to toluene molecule are larger than that of the pristine SiCNS. This supported the notion that the TM doping has an influence on the electronic properties of the SiCNS substantially, which was consistent with the previous results of Pd-doped SiCNS(Bezi Javan et al., 2016). The results indicated that the changes of electronic properties are beneficial for sensing applications.

4. Conclusions

In order to search for novel nanomaterials for toluene storage and sensing applications, the transition metals (TM = V, Nb, Ta, Cr, Mo, W, Mn, Tc, and Re) doping on SiCNS are selected. The geometric, energetic, and electronic properties of toluene adsorption on TM-doped SiCNS are calculated using the density functional theory method at B3LYP/LanL2DZ level of theory. It is found toluene molecule displays weak adsorption on the surface of pristine SiCNS (E_{ads} = -0.416 kcal/mol), whereas toluene molecule shows strong adsorption on the surface of TM-doped SiCNSs. The W_C-doped SiCNS displays the strongest interaction

with toluene molecule (E_{ads} = -51.604 kcal/mol). The ΔE_{gap} and DOSs of the TM-SiCNSs present dramatic changes after adsorption with toluene molecules. A better understanding of these interactions is achieved by NBO analysis which confirms considerable charge transfers during the adsorption of toluene molecule onto the TM-doped SiCNS. The observations show that TM-doped SiCNSs are highly sensitive toluene molecules. Thus, TM-doped

5. Acknowledgement

6. Publication Ethic

Submitted manuscripts must not have been previously published by or be under review by another print or online journal or source.

7. References

Ansari, R., Rouhi, S., Mirnezhad, M., & Aryayi, M. (2013). Stability characteristics of single-layered silicon carbide nanosheets under uniaxial compression. Physica E: *Low-Dimensional Systems and Nanostructures*, 53, 22-28. doi:10.1016/j.physe.2013.04.014

Becke, A.D., Density-functional exchange-energy approximation with correct asymptotic behavior, *Phys. Rev*. A 38 (1988) 3098-3100.

Becke, A.D., Density-functional thermochemistry. III. The role of exact exchange, *J. Chem. Phys. 98* (1993) 5648-5652.

Bezi Javan, M., Houshang Shirdel-Havar, A., Soltani, A., & Pourarian, F. (2016). Adsorption and dissociation of H_2 on Pd doped graphene-like SiC sheet. *International Journal of Hydrogen Energy*, *41*(48), 22886-22898. doi:10.1016/j.ijhydene.2016.09.081

Chabi, S., Chang, H., Xia, Y., & Zhu, Y. (2016). From graphene to silicon carbide: ultrathin silicon carbide flakes. *Nanotechnology*, 27(7), 075602.doi:10.1088/0957-4484/27/7/075602

Chiang, Y.-C., Chiang, P.-C., & Huang, C.-P. (2001). Effects of pore structure and temperature on VOC adsorption on activated carbon. Carbon, 39(4), 523-534.

Delavari, N., & Jafari, M. (2018). Electronic and optical properties of hydrogenated silicon carbide nanosheets: A DFT study. *Solid State Communications*, 275, 1-7. doi: 10.1016/j.ssc.2018.03.004

Farmanzadeh, D., & Ardehjani, N. A. (2018). Adsorption of O_3, SO_2 and NO_2 molecules on the surface of pure and Fe-doped silicon carbide nanosheets: *A computational study. Applied Surface Science*, 462, 685-692. doi: 10.1016/j.apsusc.2018.08.150

Flükiger P., Lüthi, H.P., & Portmann, S., MOLEKEL 4.3, Swiss center for scientific computing. Manno, Switzerland, 2000.

Frisch, M.J., Trucks G.W., Schlegel H.B., Scuseria G.E., Robb M.A., Cheeseman J.R., ..., Pople J.A. GAUSSIAN 09, Revision A.02, Gaussian Inc, WallingfordCT, 2009.

Goudarziafshar, H., Abdolmaleki, M., Moosavi-zare, A. R., & Soleymanabadi, H. (2018). Hydrogen storage by Ni-doped silicon carbide nanocage: *A theoretical study. Physica E: Low-Dimensional Systems and Nanostructures*, 101, 78-84.doi: 10.1016/j.physe.2018.03.001

Hay P.J., Wadt W.R., Ab initio effective core potentials for molecular calculations. Potentials for K to Au including the outermost core orbitals. *J. Chem. Phys*. 82(1985) 299-310.

Hay, P.J., Wadt W.R., Ab initio effective core potentials for molecular calculations. Potentials for the transition metal atoms Sc to Hg. *J. Chem. Phys*. 82 (1985) 270-283.

Kim, K.-H., Szulejko, J. E., Raza, N., Kumar, V., Vikrant, K., Tsang, D. C. W., … Khan, A. (2019). Identifying the best materials for the removal of airborne toluene based on performance metrics - A critical review. *Journal of Cleaner Production*, 241, 118408. doi: 10.1016/j.jclepro.2019.118408

Kunaseth, M., Poldorn, P., Junkeaw, A., Meeprasert, J., Rungnim, C., Namuangruk, S., … Jungsuttiwong, S. (2017). A DFT study of volatile organic compounds adsorption on transition metal deposited graphene. *Applied Surface Science*, 396, 1712-1718. doi: 10.1016/j.apsusc.2016.11.238

Lee, C., Yang, W., Parr, R.G., Development of the Colle-Salvetti correlation-energy formula into a functional of the electron density, *Phys. Rev*. B 37 (1988) 785-789. doi:10.1103/physrevb.37.785

Mandeep, Sharma, L., & Kakkar, R. (2018). DFT study on the adsorption of p-nitrophenol over vacancy and Pt-doped graphene sheets. *Computational and Theoretical Chemistry*, 1142, 88-96. doi: 10.1016/j.comptc.2018.08.020

Suan Sunandha Science and Technology Journal

O'boyle, N. M., Tenderholt, A. L., & Langner, K. M. (2008). cclib: A library for package-independent computational chemistry algorithms. *Journal of Computational Chemistry*, 29(5), 839-845. doi: 10.1002/jcc.20823

Su, Y., Ao, Z., Ji, Y., Li, G., & An, T. (2018). Adsorption mechanisms of different volatile organic compounds onto pristine C_2N and Al-doped C_2N monolayer: A DFT investigation. *Applied Surface Science*, 450, 484-491. doi:10.1016/j.apsusc.2018.04.157

Sun, L., & Hu, J. (2018). Adsorption of O_2 on the M doped (M=Fe, Co, Al, Cu, and Zn) SiC sheets: DFT study. *Computational Condensed Matter*, 16, doi:10.1016/j.cocom.2018.e00323

Tabtimsai, C., Kansawai P., Phoson P., Pooboontong P., & Wanno B., Adsorption of CO_2 on Ga- and B-doped silicon carbide nanosheets: A theoretical study. *The 5th International Conference on Sciences and Social Sciences 2015 (ICSSS 2015): Research and Innovation for Community and Regional Development, Rajabhat Maha Sarakham University*, Thailand, September 17-18, 2015.

Tabtimsai, C., Ruangpornvisuti, V., Tontapha, S., & Wanno, B. (2018). A DFT investigation on group 8B transition metal-doped silicon carbide nanotubes for hydrogen storage application. *Applied Surface Science*, 439, 494-505.

Wadt, W.R., Hay, P.J., Ab initio effective core potentials for molecular calculations. Potentials for main group elements Na to Bi, J. Chem. Phys. 82 (1985) 284-298. doi: 10.1063/1.448799

Wang, N., Tian, Y., Zhao, J., & Jin, P. (2016). CO oxidation catalyzed by silicon carbide (SiC) monolayer: A theoretical study. *Journal of Molecular Graphics and Modelling*, 66, 196-200. doi: 10.1016/j.jmgm.2016.04.009

Yi, F.-Y., Lin, X.-D., Chen, S.-X., & Wei, X.-Q. (2008). Adsorption of VOC on modified activated carbon fiber. *Journal of Porous Materials*, 16(5), 521-526.

Yu, L., Wang, L., Xu, W., Chen, L., Fu, M., Wu, J., & Ye, D. (2018). Adsorption of VOCs on reduced graphene oxide. *Journal of Environmental Sciences*, 67, 171-178.

Zhou, K., Ma, W., Zeng, Z., Ma, X., Xu, X., Guo, Y., … Li, L. (2019). Experimental and DFT study on the adsorption of VOCs on activated carbon/metal oxides composites. *Chemical Engineering Journal*, 372, 1122-1133. doi: 10.1016/j.cej.2019.04.218